



Reliable and energy efficient cooperative detection in wireless sensor networks

Fatma Bouabdallah^{a,b,d,*}, Nizar Bouabdallah^b, Raouf Boutaba^{a,c}

^a School of Computer Science, University of Waterloo, 200 University Avenue W., Waterloo, ON, Canada

^b INRIA, Campus Universitaire de Beaulieu, 35042 Rennes Cedex, France

^c Division of IT Convergence Engineering, Pohang University of Science and Technology (POSTECH), Pohang 790-784, Republic of Korea

^d Information Technology Department, Faculty of Computing and Information Technology, King Abdulaziz University, Jeddah, Saudi Arabia

ARTICLE INFO

Article history:

Received 22 September 2011

Received in revised form 31 October 2012

Accepted 29 November 2012

Available online 14 December 2012

Keywords:

Wireless sensor networks

Energy conservation

Routing for signal detection

Performance analysis

ABSTRACT

The efficiency of a wireless sensor network (WSN) is dependent on the level of event detection reliability it achieves, and the associated consumed amount of energy. In this work, the potential performance improvement gained by using a routing metric that reflects the quality of links in terms of detection reliability is investigated. As a first main contribution, we derive the expression of such detection reliability-aware link metric considering a realistic multi-dimensional Gaussian autoregressive (AR) model to describe information correlation within the supervised field. Such routing metric quantifies indeed the participation of each link on a path in reducing the probability of error when making final decision at the fusion center (i.e., the sink node). As a second main contribution, we propose that only the new information among the sensed information by the sensor nodes be propagated to the fusion center instead of the whole raw data. As such, the number of packets traversing the network is considerably reduced, which leads to significant energy conservation. To achieve this in a relatively easy way, we use fast filtering to aggregate data information at intermediate nodes along the path to the fusion center. Finally and as a third main contribution, we balance detection reliability and energy-efficiency by including a weighted value of the energy consumption in the expression of the detection reliability-aware link metric. This cooperative routing approach is shown to yield significant benefits to the network, by either increasing the provided QoS (i.e., the offered level of detection reliability) or allowing the network to decrease its energy consumption compared to classical noncooperative routing schemes and the cooperative routing scheme with one-dimensional correlated field.

© 2012 Elsevier B.V. All rights reserved.

1. Introduction

Energy-efficiency and reliable detection are major challenges in energy-constrained wireless sensor networks (WSNs). WSN protocols must make judicious use of the limited energy resources in order to maximize the network lifetime while respecting the specific QoS requirements of sensor applications such as the required information reliability of the detected events.

Due to the typical high density of WSNs, the sensors' measurements are often spatially correlated, so delivering all the raw data to the fusion center (i.e., sink node) may not add to the detection reliability and instead results in energy wastage. Exploiting the spatial correlation among the densely deployed sensor nodes can reduce significantly the energy consumption while ensuring the required level of detection reliability. One way to achieve this is by aggregating data at intermediate nodes. Each sensor node com-

bines the locally sensed information with the received information from the upstream nodes, and forwards the aggregate information towards the fusion center. Based on the received aggregate information resulting from the cooperative effort of the sensor nodes along the path, the fusion center makes the decision whether or not an event has occurred.

To illustrate the tradeoff between energy-efficiency and detection reliability, let us consider the sensor network example of Fig. 1. Suppose that sensor N_0 is the detection originator, which has to initiate the data reporting to the fusion center. Assume that N_0 can choose between two possible routes, R_1 and R_2 . Obviously, route R_2 enables gathering more measurements from the supervised area than R_1 since R_2 involves more sensor nodes. This, however, does not necessarily mean that R_2 is more reliable than R_1 . Indeed, data from spatially spaced sensor nodes (i.e., along R_1) may be more useful for the detection reliability than the highly correlated data from nearby located sensor nodes (i.e., along R_2).

Even more significantly, routing through R_2 instead of R_1 requires additional energy. Improving the detection reliability comes probably at the cost of increasing energy consumption.

* Corresponding author at: Information Technology Department, Faculty of Computing and Information Technology, King Abdulaziz University, Jeddah, Saudi Arabia. Tel.: +966 540714127.

E-mail address: fatma.bouabdallah@gmail.com (F. Bouabdallah).

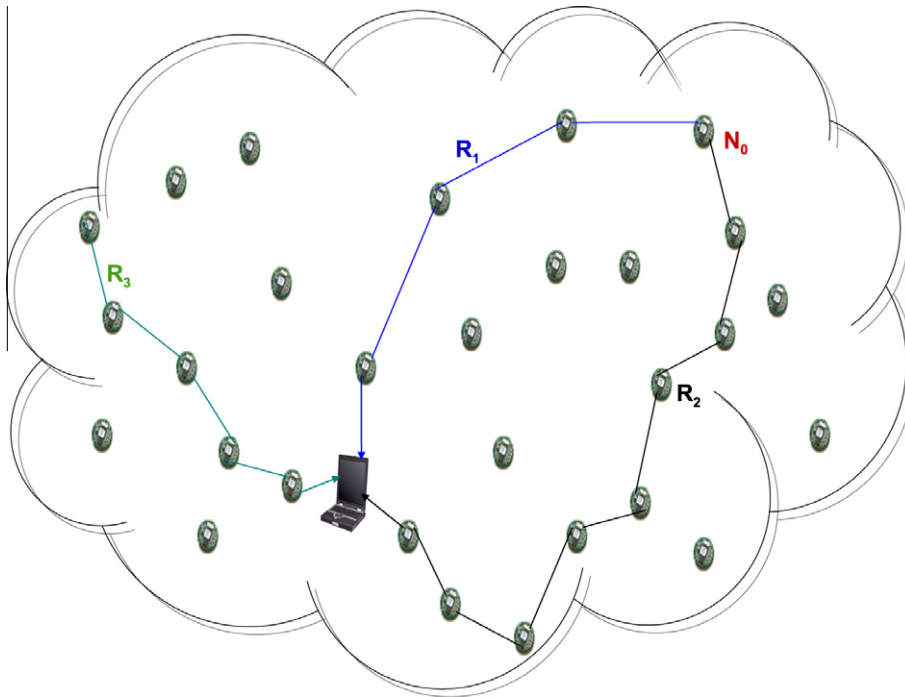


Fig. 1. Sensor network example.

Designing energy-efficient routing protocols has been addressed in several works [4–6]. However, only a few works have focused on routing for event detection. Recently, the study in [11] has shown that cooperative routing can achieve significant energy conservation compared to noncooperative routing for the same detection performance (i.e., reliability). By considering a new link metric that characterizes the detection error within one-dimensional Gauss-Markov fields, detection reliability-aware routing was introduced in [11].

In this work, deriving a routing metric, that captures the detection error induced by each link, in a realistic scenario is considered. Specifically, instead of considering a one-dimensional Gauss-Markov field, an m -order Gaussian autoregressive (AR) model is used to specify the signal correlation among the sensor nodes. In doing so, the signal sensed by a sensor node is correlated with the m upstream nodes' signals on the path and not only with the previous node. As a result, each link is not characterized by its own constant routing metric that depends only on the link length as in the one-dimensional model [11]; instead, the link metric depends on the used path for detection (i.e., which that link belongs to). In other words, the same link may have different routing metric values according to the path used for detection.

To reduce the transmission of redundant information and thus the energy consumption, we propose to aggregate data at intermediate nodes along the path to the fusion center. To achieve such cooperative routing, we use fast filtering data aggregation [16]. Moreover, to strike a balance between the energy consumption and detection performance, a weighted value of the energy consumption is added to the detection reliability-aware link metric.

The remainder of this article is organized as follows. The next section presents the state of the art as it relates to the focus of this article. Following this, Section 3 formulates the general problem and presents the system model to be studied. Section 4 derives the detection reliability-aware link metric using the generic multi-dimensional Gaussian autoregressive model. Then, the cooperative transmission through fast filtering data aggregation is presented. Section 5 extends the link metric to take into account energy consumption and Section 6 summarizes the operations of

the routing algorithm. Results are provided in Section 7, where our proposal is compared to the Minimum-Energy routing as well as to conventional noncooperative routing. The article concludes with a summary of our contributions.

2. Related work

In order to minimize the energy consumption in WSNs, several energy-efficient MAC protocols [1–3] and energy-efficient routing protocols [4,5] have been proposed in the literature. These protocols aim at decreasing the energy consumption by using sleep schedules.

Significant energy saving is achieved by such schemes, however the WSN keeps always sending redundant data. Typically, WSNs rely on the cooperative effort of the densely deployed sensor nodes to report detected events. As a result, multiple sensor nodes may report the same event. To further decrease energy consumption, several works are now focusing on the elimination of redundant information [8–10]. The reduction of the number of redundant packets can be achieved either at the data originator level (i.e., sensor nodes that detect the event) [8,9] by limiting the reporting task to a small subset of sensor nodes, or at the intermediate sensor nodes routing the information to the sink by means of aggregation mechanisms [10–12]. Data aggregation has been put forward as an essential paradigm for wireless routing in sensor networks. The idea is to combine the data coming from different sources en route. In doing so, the number of packets traversing the network is considerably reduced, which leads to significant energy conservation.

This work addresses the problem of reliable and energy-efficient detection in a spatially correlated field. Specifically, we assume that each sensor node aggregates the locally collected data and deliver it to the fusion center for optimal detection.

Energy-efficient detection in WSNs has been already studied in previous works [17–20]. However, most of these works assume conditionally independent observations. Considering correlation when gathering data results indeed in different detection performance as shown in [11].

Our work is motivated by the results presented in [11] where the authors investigated the problem of cooperative routing under the constraint of reliable detection performance. Note that the idea of cooperation on the network layer in energy-constrained wireless networks has gained much research interest over the past few years. It has been proved that conceiving a cooperative routing protocol can lead to significant energy savings [11,13–15]. Particularly, the authors in [11] adopted a cross-layer strategy that translates signal processing performance into a routing link metric. Specifically, considering a one-dimensional Gauss-Markov correlated field, a new detection reliability-aware routing metric was proposed.

This work extends the calculation of the detection reliability-aware routing metric by considering a generic multi-dimensional Gaussian autoregressive model to describe the correlated field. Such AR(m) model evaluates the cross-correlation properties of m consecutive values of a signal. Moreover, considering the AR(m) correlation model, we derive the associated aggregation strategy using the fast filtering method presented in [16].

It is worth noting that the benefits of our proposal are fulfilled especially for high reliability sensor applications. Examples of such applications include especially but not exclusively military and health applications. Indeed, sensor networks were initially deployed for military applications such as battlefield surveillance and enemy tracking. In this kind of applications, high reliability is required since the undertaken actions (embattle the army) are extremely costly. Health applications as well need great reliability. For instance, glucose level monitoring, organ monitoring and cancer detection need primarily great reliability although many additional specific challenges exist such as safety and minimal maintenance.

3. Model and problem definition

This section describes the detection process under the Bayesian framework. In our study, the sensor nodes are randomly distributed over a target field and aim at detecting the presence of specific events. Multi-hop wireless routing is used to forward data to the fusion center. The main task of the fusion center is to specify the location to be probed (for event presence) as well as the sensors that will be involved in the detection and routing processes.

The following notations are used in our analysis. $E(\cdot)$ denotes the expectation operator and $E_j(\cdot)$ is the expectation conditioned on the event H_j ; $X \sim N(\mu, \sigma^2)$ means that X is a Gaussian random variable with mean μ and variance σ^2 ; finally, V^T denotes the transpose of matrix V .

3.1. Measurement model

Assume that N_0 is the source of the detection process and that N_0, N_1, \dots, N_{n-1} are the nodes involved successively in detection and routing. $R(N_0, \dots, N_{n-1})$ represents therefore the fusion route where N_{n-1} is the fusion center. We denote by Δ_{ij} the Euclidean distance between sensors N_i and N_j . Let hypothesis H_1 denote the presence of the event within the sensor network and H_0 its absence. The observations along the route $R(N_0, \dots, N_{n-1})$ under each hypothesis can be expressed as follows:

$$\begin{aligned} H_0 : Y_i &= W_i, \quad \forall i = 0, 1, \dots, n-1, \\ H_1 : Y_i &= S_i + W_i, \quad \forall i = 0, 1, \dots, n-1, \end{aligned} \quad (1)$$

where Y_i is the observation at sensor i , and where the S_i 's are correlated Gaussian samples of the signal with $S_i \sim N(0, \sigma_S^2)$. The noise samples W_i are i.i.d. Gaussian with $W_i \sim N(0, \sigma_W^2)$.

3.2. Detection at the fusion center

The fusion center's task is to decide whether or not the event of interest has occurred in the WSN based on the observations $\{Y_i = y_i, i = 0, \dots, n-1\}$ collected from the sensor nodes along the fusion route. The optimal fusion rule which minimizes the probability of detection error for (1) is given by the likelihood ratio detector [23]:

$$\Lambda(y_0, \dots, y_{n-1}) = \begin{cases} H_1 & \text{if } \ln \frac{p_1(y_0, \dots, y_{n-1})}{p_0(y_0, \dots, y_{n-1})} \geq \tau \triangleq \ln \frac{\pi_0}{\pi_1} \\ H_0 & \text{otherwise,} \end{cases} \quad (2)$$

where $p_j(y_0, \dots, y_{n-1})$ with $j \in \{0, 1\}$, is the probability density function of the jointly Gaussian random variables under H_j , and π_j is the prior probability of H_j . It is worth noting that computing this fusion rule is an intensive and energy-consuming task [17]. In view of this, the next section expresses $\Lambda(y_0, \dots, y_{n-1})$ in a simpler way, by underlying the contribution of each link along the route in the detection performance.

3.3. Recap of Chernoff-based link metric derivation

This section recapitulates the use of Chernoff information to derive the detection reliability-aware link metric [11], and presents some of the equations from the model in [11] with brief explanations here for this paper to be self-contained. Specifically, we exhibit the use of the Chernoff information to specify the detection reliability-aware link metric that reflects the probability of detection error over a given route. Then, we show how useful is the Schweppe's recursive representation of the likelihood function in expressing the Chernoff information in an additive practical form. Using this representation, a link metric, which quantifies the participation of a given link in improving the detection performance, can be derived.

3.3.1. Chernoff information and Schweppe's recursion

In the binary hypothesis testing problem, two types of error can occur in decision making. The first type of error, known as false alarms, occurs when H_0 is true and instead H_1 is declared. The associated conditional probability of false alarms is P_F . The second type of error, a miss, occurs when H_0 is declared true although H_1 is present. The associated probability of error is known as the probability of miss P_M . Then, we have:

$$P_F = P\{\text{decide } H_1 | H_0 \text{ present}\} \quad (3)$$

$$P_M = P\{\text{decide } H_0 | H_1 \text{ present}\}. \quad (4)$$

Thus the average probability of detection error is:

$$\mathbf{P}_E = \pi_0 P_F + \pi_1 P_M \quad (5)$$

The Chernoff's asymptotic bound on the best achievable Bayes probability of error \mathbf{P}_E is given by [21]:

$$\mathbf{P}_E \leq \pi_0^{1-s} \pi_1^s e^{\mu(s)} \quad (6)$$

where $\mu(s)$ is the cumulant generating function of the loglikelihood ratio under H_0 , i.e.,

$$\mu(s) = \ln E_0 \left\{ e^{s \ln \frac{p_1(y_0, \dots, y_{n-1})}{p_0(y_0, \dots, y_{n-1})}} \right\}, \quad 0 \leq s \leq 1. \quad (7)$$

Chernoff's asymptotic bound gives exponentially decreasing bound on the probability of error of the optimal Bayesian decision rule. Then, the Chernoff information [22] is defined as follows:

$$\mathbf{C}(p_0, p_1) \triangleq \sup_{0 \leq s \leq 1} \{-\mu(s)\} \quad (8)$$

Chernoff information thus provides the best Bayesian exponent error. For more details, readers are referred to [11,21].

The Chernoff information can be calculated using the Scheppe's recursive representation of the likelihood function [26]. The major advantage of this approach compared with the conventional procedure [21] [pp. 89–90] for the calculation of Chernoff information is its simplicity and usefulness. Indeed, Scheppe's approach quantifies the contribution of each link in the P_E of a route.

Accordingly, the loglikelihood up to the i th observation along a route can be expressed as follows:

$$\ln p_1(y_0, \dots, y_i) = \ln p_1(y_0, \dots, y_{i-1}) - \frac{1}{2} \ln (2\pi\sigma_{\text{innov},i}^2) - \frac{1}{2} \times \frac{\tilde{y}_i^2}{\sigma_{\text{innov},i}^2} \quad (9)$$

where $\tilde{y}_i \triangleq y_i - \hat{y}_i$, $\hat{y}_i = E_1\{Y_i|y_0, \dots, y_{i-1}\}$ is the minimum mean square error (MMSE) prediction of Y_i conditioned on the event $\{Y_0, \dots, Y_{i-1}\}$ and $\sigma_{\text{innov},i}^2 = E_1\{\tilde{y}_i^2\}$ is the MMSE of the predictor.

Thus, the loglikelihood of the observations under H_1 can be deduced by recursively evaluating (9). Hence, we get

$$\ln p_1(y_0, \dots, y_{n-1}) = -\frac{1}{2} \sum_{i=0}^{n-1} \ln (2\pi\sigma_{\text{innov},i}^2) - \frac{1}{2} \sum_{i=0}^{n-1} \frac{\tilde{y}_i^2}{\sigma_{\text{innov},i}^2} \quad (10)$$

Now, in order to get $\mu(s)$, we need to evaluate $p_0(y_0, \dots, y_{n-1})$, which can be seen as the standard product form of the independent Gaussian variables $w_i (i = 0, \dots, n - 1)$, thereby

$$\begin{aligned} \ln p_0(y_0, \dots, y_{n-1}) &= \ln \prod_{i=0}^{n-1} p_0(y_i) = \ln \prod_{i=0}^{n-1} p(w_i) \\ &= -\frac{n}{2} \ln (2\pi\sigma_w^2) - \frac{1}{2} \sum_{i=0}^{n-1} \frac{y_i^2}{\sigma_w^2} \end{aligned} \quad (11)$$

Finally, using (10) and (11), we get Eq. (12).

$$\begin{aligned} \mu(s) &= \ln E_0 \left\{ \exp \left[s \left(-\frac{1}{2} \sum_{i=0}^{n-1} \ln (2\pi\sigma_{\text{innov},i}^2) - \frac{1}{2} \sum_{i=0}^{n-1} \frac{\tilde{y}_i^2}{\sigma_{\text{innov},i}^2} \right. \right. \right. \\ &\quad \left. \left. \left. + \frac{n}{2} \ln (2\pi\sigma_w^2) + \frac{1}{2} \sum_{i=0}^{n-1} \frac{Y_i^2}{\sigma_w^2} \right) \right] \right\}. \end{aligned} \quad (12)$$

3.3.2. The link metric

In [11], the authors derived the expression of detection reliability-aware link metric, which characterizes the contribution of each link to the overall P_E of a route. To do so, the authors considered three approximations, which can be easily justified for large n and at high SNR [11]. Accordingly, $p_0(y_0, \dots, y_{n-1})$ can be expressed as follows:

$$\ln p_0(y_0, \dots, y_{n-1}) = -\frac{n}{2} (\ln (2\pi\sigma_w^2) + 1) \quad (13)$$

and thus the cumulant generating function is approximately equal to:

$$\mu(s) \approx s \left\{ -\sum_{i=0}^{n-1} \frac{1}{2} \ln (\sigma_{\text{innov},i}^2) + \frac{n}{2} \ln (\sigma_w^2 + 1) + \frac{n}{2} \right\}. \quad (14)$$

Hence, combining (6) and (14), we get:

$$P_E \leq B_c = \pi_0^{1-s} \pi_1^s e^{-s \left\{ \sum_{i=0}^{n-1} \left(\frac{1}{2} \ln \frac{\sigma_{\text{innov},i}^2}{\sigma_w^2} - \frac{1}{2} \right) \right\}} \quad (15)$$

where $0 \leq s \leq 1$.

Finally, since at high SNR, $\sigma_{\text{innov},i}^2/\sigma_w^2 \gg 1$, the Chernoff information is obtained by putting $s = 1$ in (8), and is approximately given by:

$$C(p_0, p_1) \approx \sum_{i=0}^{n-1} \left(\frac{1}{2} \ln \frac{\sigma_{\text{innov},i}^2}{\sigma_w^2} - \frac{1}{2} \right) \approx \sum_{i=0}^{n-1} \frac{1}{2} \ln \frac{\sigma_{\text{innov},i}^2}{\sigma_w^2} \quad (16)$$

Now, focusing on the new additive form of the Chernoff information, we can identify the role of each link in improving the detection performance. In fact, (16) and (6) point out that the term:

$$\bar{C}_i = \frac{1}{2} \ln \frac{\sigma_{\text{innov},i}^2}{\sigma_w^2} \quad (17)$$

quantifies the participation of the i th link in the P_E of a route. In other words, \bar{C}_i quantifies the reduction in P_E achieved by involving N_i in the detection process. \bar{C}_i is the proposed link metric which can be interpreted as the amount of useful information acquired by collecting a sample from node N_i . Therefore, the optimal route is the one that provides the maximum amount of useful information leading to the maximum reduction in the probability of error during decision making at the fusion center.

In view of this and as a first main contribution of this work, we derive the expression of the detection reliability-aware link metric considering a more realistic m -order Gaussian autoregressive correlated field instead of the one-dimensional Gauss-Markov field. In doing so, the signal sensed by a sensor node is correlated with the m upstream nodes' signals on the path and not only with the previous node. Moreover, \bar{C}_i suggests that only the relevant information should be propagated to the fusion center instead of the entire raw data. Based on this observation and as a second main contribution, we use fast filtering to achieve aggregation. Accordingly, only innovations regarding the sensed information are transmitted between successive nodes on the fusion route.

4. Cooperative routing for the detection of a Gaussian autoregressive correlated field

In the remainder of this paper we assume that the correlation is described by the general class of Gaussian autoregressive model.

4.1. Autoregressive correlation model

Autoregressive is a term derived from time series analysis which assumes that observations are related to their own past values through one, two, or a higher order autoregressive process. Frequently, we find that the value of a sensed signal at particular point in time is highly correlated with the values which precede it. An autoregressive correlation structure indicates that two observations taken close in time and/or space tend to be more highly correlated than two observations taken far apart in time and/or space. An m -order autoregressive model considers the relationship between m consecutive values of a signal by evaluating the cross-correlation properties between them.

We would like to emphasize that the inner nature of the multi-dimension Gaussian autoregressive model make it realistic especially for event driven sensor applications. In event-driven reporting, the sensor network is tailored to detect the occurrence of a pre-specified abnormal event within the sensor field. Such abnormal events are non local in the temporal and spatial dimensions. Indeed, in the temporal dimension, abnormal events are usually causal meaning that future information is inevitably correlated to past ones. Moreover, abnormal events can easily be detected by multiple sensors which justifies the spatial correlation.

The multi-dimension autoregressive model assumes that observations are related to their own past values. Frequently, two observations of the same sensed phenomena taken at two different points in time and/or space are correlated. The correlation level depends mainly on how closer (in time and/or space) the observations are. Indeed, the closer the observations (in time and/or

space) the higher the correlation. For instance, let's consider the trigger of a fire event in a farm where enough sensors are scattered. Future observations of the same sensor are inevitably correlated to past ones. Moreover, two observations of two distinct sensors equally spaced from the source event are surely correlated.

Under the Gaussian autoregressive model, the dynamics of signal sample S_i at node N_i is described by the following state-space model:

$$\begin{cases} S_i + \alpha_{i(i-1)}S_{i-1} + \dots + \alpha_{i(i-m)}S_{i-m} = e_i, & i = 0, 1, \dots, n-1 \\ \alpha_{ij} = -e^{-A\Delta_{ij}}, & j = 1, \dots, m \end{cases} \quad (18)$$

where m denotes the correlation order, A is the correlation parameter and $e_i \sim N(0, \sigma_e^2)$ is the driving process. The $\{e_i\}$, $i = 0, \dots, n-1$ are i.i.d. Gaussian random variables with zero means and variances σ_e^2 . e_i is uncorrelated with W_i .

Recall that under the event H_1 , we have:

$$Y_i = S_i + W_i, \quad (19)$$

Equations in (18) and (19) can be also expressed in the polynomial form as follows:

$$A_i(z^{-1})Y_i = e_i + A_i(z^{-1})W_i \quad (20)$$

where

$$A_i(z^{-1}) = 1 + \alpha_{i1}z^{-1} + \dots + \alpha_{im}z^{-m} \quad (21)$$

with z^{-1} is the unit delay operator.

4.2. Link metric evaluation

In order to evaluate the link metric (17) under the Gaussian autoregressive model (18), we have to express the variance $\sigma_{\text{innov},i}^2$ of the innovation process \tilde{y}_i . Inspired from [16], the innovation process \tilde{y}_i can be obtained recursively by using the triangular decomposition of symmetric matrices as described in [25].

Define, for this purpose, the stochastic process:

$$\gamma(i) = A_i(z^{-1})Y_i = e_i + A_i(z^{-1})W_i \quad (22)$$

The autocorrelations of $\gamma(i)$ are given by:

$$r_{\gamma(i)}(j) = E[\gamma(i)\gamma(i-j)] = r_{\gamma(i-j)}(-j) \quad (23)$$

which yields:

$$r_{\gamma(i)}(j) = \begin{cases} \sigma_W^2 \sum_{k=0}^{\min((i-1),m)} \alpha_{i(i-k)}^2 + \sigma_e^2, & \text{if } j = 0 \\ \sigma_W^2 \sum_{k=0}^n \alpha_{i(i-j-k)} \alpha_{i-j-k}, & \text{if } j = 1, \dots, m \\ 0, & \text{if } j > m \end{cases} \quad (24)$$

where $n = \min((m-j), (i-j-1))$. According to [16], it has been shown that $\gamma(i)$ can be considered as a time-varying moving average process driven by the innovation \tilde{y}_i .

Let us now define the vector:

$$\Gamma(i) = [\gamma(0)\gamma(1) \dots \gamma(i)]^T \quad (25)$$

whose covariance matrix is $R_\gamma(i)$.

Based on (24), $R_\gamma(i)$ exhibits a symmetric structure, i.e.,

$$R_\gamma(i) = E[\Gamma(i)\Gamma^T(i)] = [R_{pq}] \quad (26)$$

where

$$R_{pq} = \begin{cases} r_{\gamma(p)}(p-q), & \text{if } p > q \\ r_{\gamma(q)}(q-p), & \text{if } q > p \end{cases}$$

Using (24), $R_{pq} = 0$ for $q > p+m$ or $p > q+m$. Since $R_\gamma(i)$ is symmetric, $R_\gamma(i)$ admits the following unique decomposition:

$$R_\gamma(i) = L_\gamma(i)D_\gamma(i)L_\gamma(i)^T \quad (27)$$

where $L_\gamma(i)$ is lower triangular matrix:

$$L_\gamma(i) = \begin{bmatrix} 1 & 0 & \dots & 0 & 0 & \dots & 0 \\ l_1(1) & 1 & \dots & 0 & 0 & \dots & 0 \\ \vdots & \ddots & \dots & \vdots & \vdots & \dots & \vdots \\ l_m(m) & \dots & l_1(m) & 1 & 0 & \dots & 0 \\ 0 & l_m(m+1) & \dots & l_1(m+1) & 1 & \dots & 0 \\ \vdots & \vdots & \dots & \vdots & \vdots & \dots & \vdots \\ 0 & 0 & \dots & l_m(i) & \dots & l_1(i) & 1 \end{bmatrix} \quad (28)$$

and

$$D_\gamma(i) = \text{diag}[d_0 d_1 \dots d_i] \quad (29)$$

Using the triangular decomposition of symmetric matrices described in [25], $L_\gamma(i)$ and $D_\gamma(i)$ can be recursively computed. According to [16,24], the process $\gamma(i)$ can thus be described by the time-varying moving-average model

$$\gamma(i) = \tilde{y}_i + l_1(i) = \tilde{y}_{i-1} + \dots + l_m(i)\tilde{y}_{i-m} \quad (30)$$

driven by the innovation \tilde{y}_i whose variance is

$$E[\tilde{y}_i^2] = \sigma_{\text{innov},i}^2 = d_i \quad (31)$$

It is worth noting that $R_\gamma(i)$ elements (see Eq. 24) only depends on α_{ij} where $\alpha_{ij} = -e^{-A\Delta_{ij}}$. Note also that Δ_{ij} is the Euclidean distance between sensors N_i and N_j . Thereby, $R_\gamma(i)$ entries as well as d_i are expressed only as a function of the Euclidean distance separating sensor nodes. Thus, there is no need of sensors' observations in order to evaluate each link metric. In other words, the cost associated with each link ($N_i N_j$) only depends on the euclidean distances separating N_j from the m previous nodes in the detection path, where m is the correlation order.

Note that, authors in [11] were able to derive the reliability-aware link metric as a function of the link length considering a one-dimensional correlation model. Our work extends the one-dimension Gauss-Markov model by considering a generic multi-dimensional Gaussian Autoregressive model to describe the correlated field. As a result, each link is not characterized by its own constant routing metric that depends only on the link length as in the one-dimensional model [11]; instead, the link metric depends on the m upstream links' lengths. Consequently, work in [11] can be seen as a special case where m equals 1.

4.3. Fast aggregation algorithm

Data aggregation is an efficient technique to reduce energy consumption in WSNs by avoiding redundant transmissions. This can be done of course by means of standard Kalman filtering or through fast filtering. Fast filtering ensures the same numerical robustness as Kalman filtering but with higher computational efficiency [16]. In fact, the computational complexity of fast filtering increases only linearly with the order of the AR process. A schematic of the fast-filtering based aggregation is shown in Fig. 2.

According to Schweppe's recursion (9), the loglikelihood up to the i th sensor can be calculated recursively based on its own measurement and on the information gathered by sensor N_{i-1} . Therefore, in order to compute its own likelihood function, node N_i needs the following three cumulative quantities:

1. The accumulated likelihood function $ll_{i-1} = \ln p_1(y_0, \dots, y_{i-1})$.
2. The mean-square error of the prediction $\sigma_{\text{innov},i}^2$.
3. The measurement innovation \tilde{y}_i .

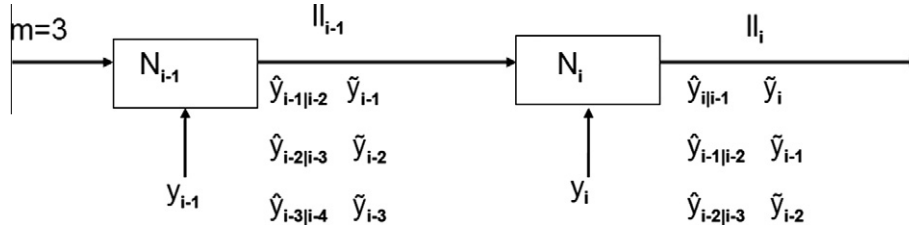


Fig. 2. An illustrative schematic of the proposed data aggregation.

Thus, the aggregation algorithm performed by each node on the fusion route can be described as follows:

1. Initialization at N_0 :

- (a) $l_{-1} = 0$,
- (b) $\hat{y}_0 = y(0)$,
- (c) $d_0 = \sigma_w^2 + \sigma_e^2$,
- (d) $\forall i = -1, \dots, -m \Rightarrow \hat{y}_{0i} = 0$ and $\tilde{y}_i = 0$

2. Compute $\gamma(i)$:

$$\gamma(i) = y(i) + \alpha_1 y(i-1) + \dots + \alpha_m y(i-m)$$

$$y(i-j) = \hat{y}_{i-j} + \hat{y}_{i-j|j-1} \quad \text{for } j = 1, \dots, m, \quad (32)$$

3. Compute the coefficients $l_1(i), \dots, l_m(i)$ using [25]

4. Compute the innovation \tilde{y}_i :

$$\tilde{y}_i = \gamma(i) - l_1(i)\tilde{y}_{i-1} - \dots - l_m(i)\tilde{y}_{i-m} \quad (33)$$

5. Compute the mean-square error of the prediction $\sigma_{\text{innov},i}^2$ by means of [25]

$$\sigma_{\text{innov},i}^2 = d_i \quad (34)$$

6. Compute l_i based on (9)

7. Send to N_{i+1} :

- (a) l_i
- (b) $\hat{y}_j, \hat{y}_{jj-1}, \forall j = i, \dots, i-m$

Finally, we can conclude that owing to our aggregation strategy only the innovations and the predicted measurements of the m -previous sensors are propagated between successive nodes in the fusion route until reaching the sink node where the fusion rule is computed according to (2).

4.4. Fusion rule computing

Under the binary hypothesis testing problem, the most common approach to decide whether an event is present or not, is the likelihood ratio test (2). It is for the recursive calculation of this quantity ($\Lambda(y_0, \dots, y_{n-1})$) that the Scheweppe's recursion along with the fast aggregation come to their own. In fact, once the detection process is accomplished, the fusion center can easily make the right decision by combining the results of our cooperative routing (9) (see Step 6 in 4.3) and (13).

5. Energy consumption analysis

This section evaluates the amount of energy consumed following the detection process, i.e., the energy needed to report the sensed information through the selected fusion route.

In this work, the detection process is initiated at a specific sensor node following an explicit demand from the sink node. In this case, each intermediate sensor on the selected fusion route cannot send its own information unless it receives the data information from its predecessor. As such, competitive access to the common channel happens only when multiple detection queries are

initiated simultaneously by the sink node. In such a case, we assume that the access to the medium among competing nodes is arbitrated by the well known CSMA/CA technique.

We use the following energy consumption model to describe energy consumed at node N_{i-1} when transmitting/receiving a packet of S bits to/from node N_i :

$$E_{i-1}^{\text{trans}}(S) = S \times (P_t + P_0^\beta \Delta_{(i-1)i})$$

$$E^{\text{rec}}(S) = S \times P_r \quad (35)$$

where P_t and P_r correspond to transmit and receive circuitry power consumption, and P_0 is the reference transmit amplifier power consumption per unit of distance.

Consequently, the energy consumed by the network in forwarding a packet through the link (N_{i-1}, N_i) is given by:

$$E_{(i-1)i} = \bar{N}_c(N_{i-1}, N_i) \times E_{i-1}^{\text{trans}}(\text{DATA}) + E_i^{\text{trans}}(\text{ACK}) \times 1_{|N_i \neq \text{Sink}}$$

$$+ |H(N_{i-1})| \times E^{\text{rec}}(\text{DATA}) \times \bar{N}_c(N_{i-1}, N_i) + |H(N_i)| \times E^{\text{rec}}(\text{ACK}) \quad (36)$$

where $|H(N_i)|$ is the number of nodes that overhears the transmission of N_i and $\bar{N}_c(N_{i-1}, N_i)$ denotes the average number of transmission attempts experienced by a packet sent from N_{i-1} to be successfully received by N_i . $\bar{N}_c(N_{i-1}, N_i)$ can be calculated as follows. Let $N_c(N_{i-1}, N_i)$ be a random variable representing the number of unsuccessful transmissions experienced by a packet before being successfully transmitted from N_{i-1} to N_i . We denote by $\beta(N_{i-1}, N_i)$ the probability that a transmission attempt from N_{i-1} to N_i be unsuccessful. $N_c(N_{i-1}, N_i)$ is a geometric random variable and thus we have:

$$E[N_c(N_{i-1}, N_i)] = \bar{N}_c(N_{i-1}, N_i) = \frac{\beta(N_{i-1}, N_i)}{1 - \beta(N_{i-1}, N_i)} \quad (37)$$

Note that $\beta(N_{i-1}, N_i)$ can be determined according to [7].

It is important to point out that in a conventional noncooperative routing, all the sensor nodes involved in the detection process should send their measurements individually to the fusion center through the multi-hop path, requiring thus a total energy consumption of:

$$E_R^{\text{nc}} = \sum_{i=1}^{n-1} \sum_{j=i}^{n-1} E_{(j-1)j} \quad (38)$$

which grows in the order of $O(n^2)$. Enabling our fast aggregation strategy reduces considerably the energy consumption. According to our cooperative routing, the energy consumption is:

$$E_R^{\text{c}} = \sum_{i=1}^{n-1} \max(m, i) \times E_{(i-1)i} \quad (39)$$

where m is the correlation order. We can see that enabling our cooperative routing scheme, the energy consumption E_R^{c} grows in the order of $O(n)$ instead of $O(n^2)$.

It is worth noting that using our data aggregation mechanism, each node has to send at most m packets to its successor on the fusion route. However, under the noncooperative strategy, the energy consumption of each node depends mainly on its position on the fusion route. Typically, the closer a node to the fusion center is, the more energy it consumes to forward the measurements of all the previous nodes on the route. Thus, considering noncooperative routing, the average energy consumed per sensor node following a detection process query increases with the increase of the network size. Using cooperative routing, the energy consumption per node remains instead practically constant regardless of the network size. This reveals indeed another major strength of our cooperative routing.

6. Cooperative routing operations

This section describes how the fusion route between the detection originator node (i.e., designated by the sink node) and the fusion center is calculated.

The problem of finding the best path is a critical issue in the design and analysis of networks. Most routing problems can be solved as shortest path problems once an appropriate additive cost is assigned to each link. The chosen link metric may reflect the system resources that are consumed when this link is used such as the delay, energy consumption or detection performance.

Our cooperative routing relies indeed on the shortest path routing to determine the path enabling the lowest detection error. Typically, the Fast-Dijkstra algorithm is applied using the detection reliability-aware cost metric (17). Specifically, the cost $M_{i(i+1)}$ associated to the link (N_i, N_{i+1}) is given by:

$$M_{i(i+1)} = C_i \quad (40)$$

where C_i is given by (17).

As a distinguishing feature from classic shortest path routing, multiple costs can be associated to each link. Each link is no more characterized by its own routing cost metric that depends only on the specific link properties such as the current load; instead, the link cost depends on the path used for detection. In other words, the same link may have different costs according to the fusion route used for detection which is a computational and time consuming task. Such constraints, can be easily justified in high reliability sensor applications. For instance, the primary requirement of military and health applications is reliability. In these applications solar energy harnessing and body heat energy harnessing can respectively resolve the extra energy consumption problem. Our proposal is especially designed for high reliability sensor applications which tolerate extra delay and energy consumption.

In our work, different reliability-aware link metrics are needed for different event initiators (sources) and for different paths. To meet this requirement, we propose the modified Fast-Dijkstra algorithm depicted in Fig. 3. In this case, the link costs are not calculated in advance. Instead, the costs of links are computed during the discovery of the best path since the link costs depend on the selected path.

It is worth noting that the first main contribution of our work is to derive the expression of the detection reliability-aware link metric considering a more realistic m -order Gaussian autoregressive correlated field instead of the one-dimensional Gauss-Markov field. Once we defined the appropriate cost for each link, we suppose that the routing problem can be solved using any shortest path routing algorithm. However, since in our analysis multiple costs can be associated with each link, we proposed Fast-Dijkstra algorithm as an example showing how to deal with such constraint. This work demonstrates the potential of these concepts,

and provides a baseline for measuring the performance of other more sophisticated routing protocols.

To balance between the detection reliability and the energy consumption, we can include the energy consumption in the link cost as follows:

$$M_{i(i+1)} = (1 - \omega)E_{i(i+1)}^c + \omega C_i \quad (41)$$

with

$$E_{i(i+1)}^c = \max(m, (i + 1))E_{i(i+1)} \quad (42)$$

where $E_{i(i+1)}^c$ is the energy consumed over the link (N_i, N_{i+1}) of the fusion route and $0 \leq \omega \leq 1$ is a weighting factor that enables to strike a balance between the detection performance and energy constraint. Note that setting $\omega = 1$, we get the pure detection reliability-aware metric as in (40).

In the next section, our cooperative routing scheme will be compared to the noncooperative routing as well as to the Minimum-Energy routing. In the latter case, the cost of each link represents the amount of energy consumed when using such link, i.e.,

$$M_{i(i+1)} = E_{i(i+1)} \quad (43)$$

where $E_{i(i+1)}$ is given by (36). The resulting path enables the lowest energy consumption between the detection originator and the fusion center.

7. Performance evaluation

In this section, we study the efficiency of our cooperative routing strategy. Specifically, we compare our detection reliability-aware routing scheme to the conventional Minimum-Energy routing and the noncooperative routing schemes in terms of detection reliability and energy consumption.

In our analysis, the sensor nodes are randomly deployed in a square field 2×2 . The sink node is located at the center. Sensors within a distance of 0.3 are assumed to be capable of direct communications. The originator node N_0 is chosen randomly. It is worth noting that the Fast-Dijkstra algorithm used to evaluate the performance of our proposal mainly needs the topology of our sensor network. In other words, finding the shortest path between the originator node N_0 and the SINK relies on the network topology (sensor nodes' placement) and the $SNR = \frac{\sigma_s^2}{\sigma_w^2}$. The parameters setting used in our analysis are listed in Table 1.

7.1. Optimal Path Selection: detection reliability-aware routing vs. Minimum-Energy routing

Fig. 4 shows the selected route between the originator node N_0 and the fusion center S according to the detection reliability-aware routing and Minimum-Energy routing strategies for a network consisting of $N = 200$ sensor nodes and with $m = 3$. This is a representative example to illustrate the difference between the two routing strategies. Accordingly two main findings can be stated:

- The Minimum-Energy routing uses a direct path consisting of short multi-hop links to connect the originator node to the fusion center (see Fig. 4a). Using such path minimizes indeed the energy consumption, but probably at the cost of reduced detection reliability.
- To increase the detection reliability, our cooperative routing scheme selects longer paths than the Minimum-Energy routing. Indeed, as more sensor nodes participate in the detection process, the reliability of the received information at the sink node increases. The maximum detection reliability is obtained when the fusion route depicted in Fig. 4c is used. To achieve this, ω is

```

function Fast-Dijkstra(Graph, source, Sink, Distance):
  for each vertex v in Graph: // Initializations
    cost[v] := infinity // Unknown cost function from source to v
    previous[v] := undefined
  end for
  cost[source] := 0 // Cost from source to source
  NotSeen := copy(Graph) // All nodes in the graph are unoptimized
  while NotSeen is not empty: // The main loop
    u := extract_min(NotSeen)
    if u=Sink
      break
    end if
    for each neighbor v of u and v ∈ NotSeen // where v has not yet been removed from NotSeen.
      R:= CovMatrix(u, v, previous, Distance)
      D := TriangularDecomp(R)
      link_cost(u, v) := ComputeCost(u, v, D, Distance)
      alt := cost[u] + link_cost(u, v)
      if alt < cost[v]
        cost[v] := alt
        previous[v] := u
      end if
    end for
  end while
  return previous

```

Fig. 3. Fast-Dijkstra algorithm.

Table 1
Parameters setting

Transmit power	24.75 mW
Receive power	13.5 mW
Reference amplifier power	1 W
$SNR = \frac{\sigma_s^2}{\sigma_w^2}$	15 dB
π_0	0.75
A	0.1

set equal to 1 in (41). Visiting additional nodes in the fusion route does not improve the reliability detection while it increases probably the energy consumption. To balance between detection reliability and energy consumption, ω can be varied between [0, 1]. For instance, Fig. 4b shows the fusion route for $\omega = 0.5$.

7.2. Detection reliability-aware routing evaluation

The performance of our cooperative routing scheme varies with the weighting factor ω , the correlation order m and the network size N . Hereafter, we analyze the impact of these parameters on the efficiency of our proposal. To achieve this, we consider the following performance metrics:

- Number of hops: is the average length of a fusion route.
- Energy consumption (J): is the average energy consumed to perform detection through a fusion route.
- Chernoff information: is the average amount of useful information acquired at the sink node by collecting observations along a fusion route (given by (8)).
- Chernoff efficiency: is the average Chernoff information divided by the energy consumption. This metric reflects the efficiency of the routing scheme in terms of both detection reliability and energy consumption.
- Detection error probability: measures the accuracy of the fusion center decision based on the gathered measurements from each node in the fusion route (given by (15)).
- Cooperative ratio: is the relative increase in energy consumption of the noncooperative routing scheme compared to the cooperative routing scheme (E_R^{nc}/E_R^c).

The results provided hereafter are averaged over 100 random network topologies for each network size N .

7.2.1. Impact of the weight ω

Let us first focus on the impact of ω on the performance of our cooperative routing scheme considering the case where $N = 150$ and $m = 3$.

Fig. 5 shows the average number of hops and the energy consumption as function of ω . We can see that the fusion route length increases with ω from $n = 7.8$ when $\omega = 0$ to $n = 41$ when $\omega = 1$. This is because, increasing ω increases the impact of the detection reliability over the energy consumption in the link cost. Typically, setting $\omega = 1$ returns the path with the highest detection reliability, whereas $\omega = 0$ leads to the path with minimum energy consumption. As stated before, increasing the detection reliability implies the reception of additional information at the sink node. This means that additional nodes have to participate in the detection process, which results in an increase of the fusion route length. In this regard, the increase of the detection reliability is achieved at the cost of longer paths and thus additional energy consumption. Note that the energy consumption increased fivefold between $\omega = 0$ and $\omega = 1$. Indeed, when $\omega = 0$, the energy consumption equals 3 J and reaches 15 J when $\omega = 1$.

The increase of the detection reliability with ω is illustrated in Figs. 6 and 7 where the Chernoff information increases and the detection error P_E decreases, respectively with ω . Indeed, as more nodes are involved in the detection process, the additive Chernoff information grows leading thus to more accurate decision at the fusion center. Note that the probability of detection error decreases by 85% between $\omega = 0$ and $\omega = 1$.

Fig. 6 shows the Chernoff efficiency curve, which exhibits a convex pace due to the different growth speed of the energy consumption and the Chernoff information with ω . Specifically, up to $\omega = 0.3$, the Chernoff information growth dominates the one of the energy consumption. Whereas, when $\omega > 0.3$, the roles are reversed. The maximum Chernoff efficiency is reached when $\omega = 0.3$ and equals almost 3.

Finally, Fig. 7 shows the relative improvement in terms of energy-efficiency of our cooperative routing scheme compared to the noncooperative one, which increases with ω . As expected, the longer a fusion route (see Fig. 5) the more important the cooperative ratio

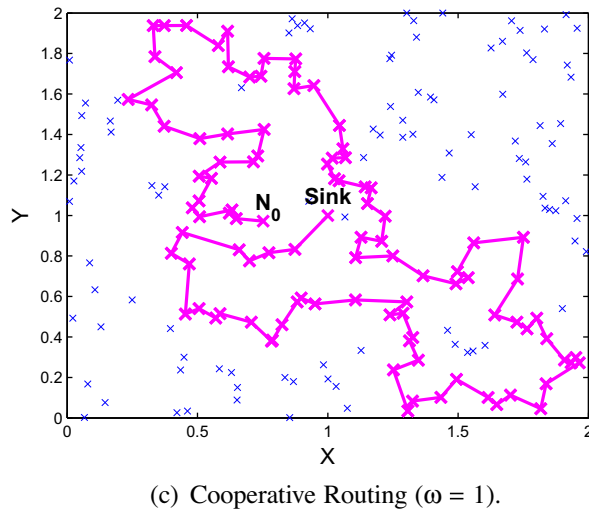
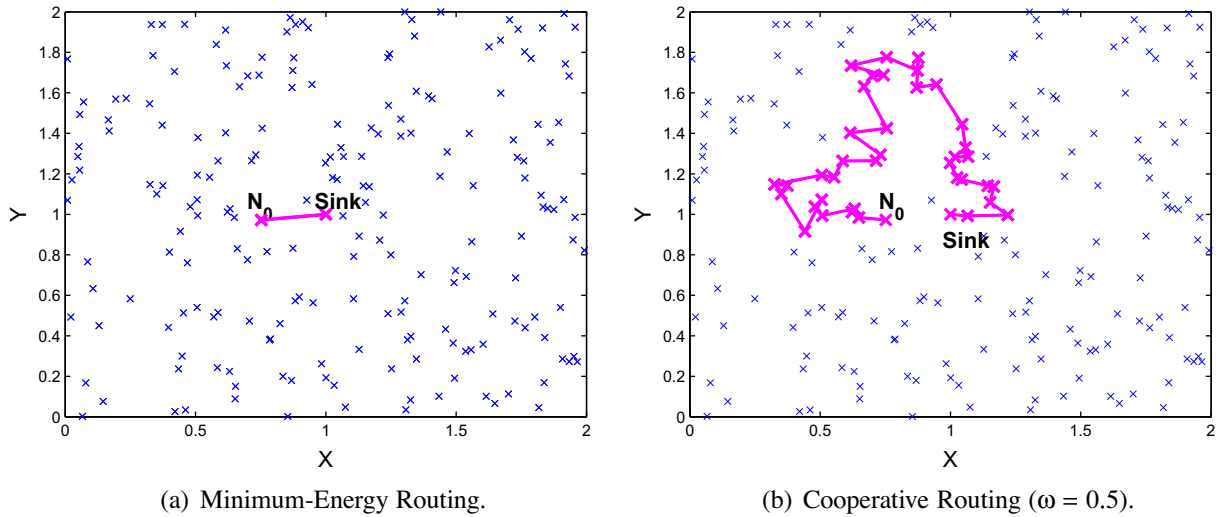


Fig. 4. The shortest path route from node N_0 to the fusion center S.

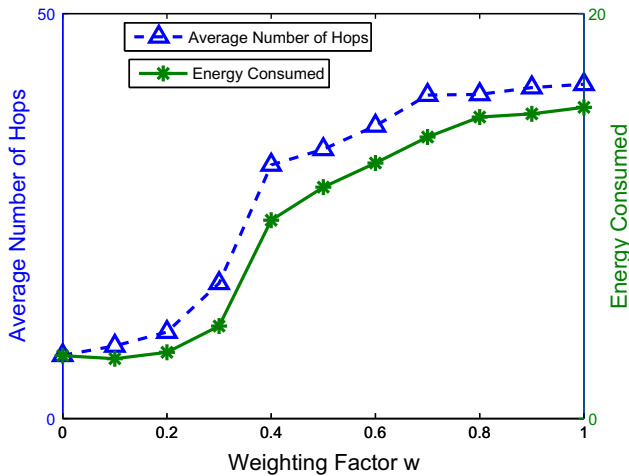


Fig. 5. Average number of hops vs. energy consumed.

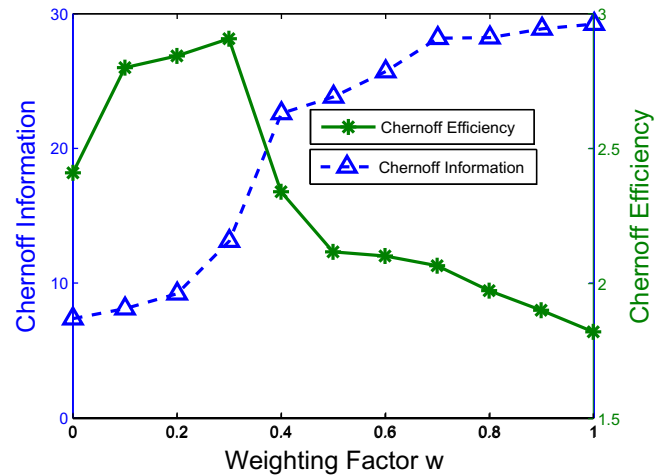


Fig. 6. Chernoff information vs. Chernoff efficiency.

(see Fig. 7). Adding nodes to the fusion route increases indeed the relative inefficiency of the noncooperative routing. Recall that, the energy consumption with the noncooperative routing increases in

the order $O(n^2)$, whereas it is only $O(n)$ with our cooperative routing. Note that, the energy consumption of the noncooperative routing scheme is almost eightfold the energy consumption of the cooperative routing scheme when ω is set equal to 1.

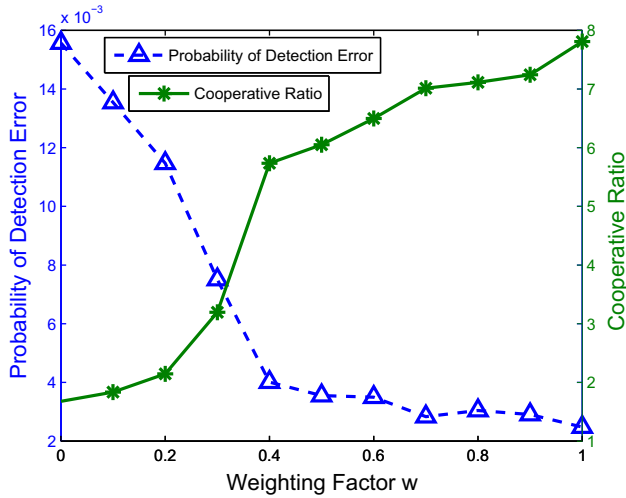


Fig. 7. Probability of detection error vs. cooperative ratio.

7.2.2. Impact of the correlation order m

The next set of experiments explores the impact of the correlation order m on the network performance when $N = 150$ and

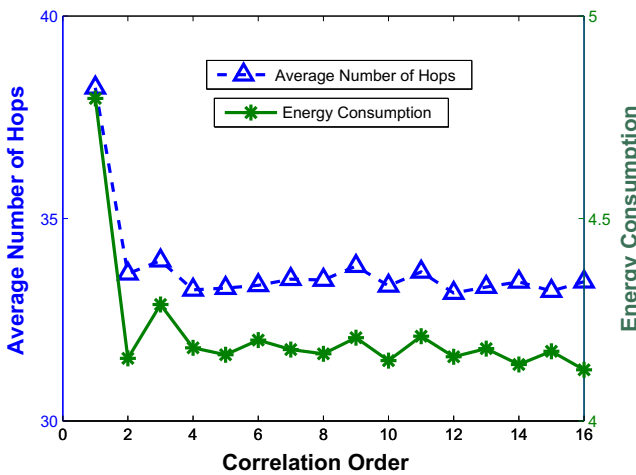
Table 2

Comparison between our cooperative routing and the min-energy routing.

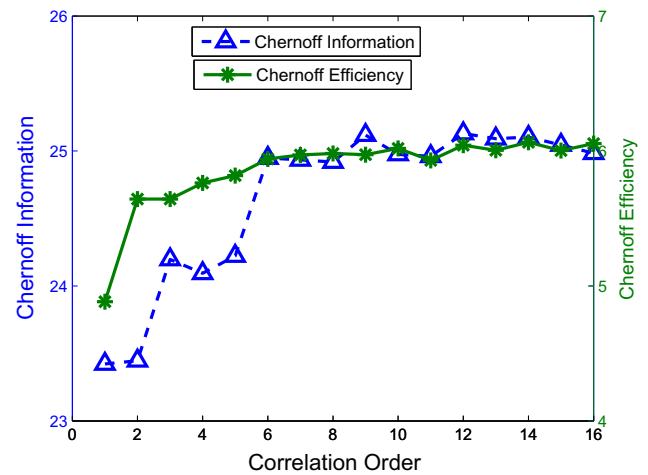
	Chernoff efficiency	Prob. detection error
Min-energy routing	1.27	1.98×10^{-4}
Cooperative routing	Min value = 4.88	Max value = 1.68×10^{-11}

$\omega = 0.6$. It is worth noting that putting $m = 1$, we simply get all the results relative to the one-dimension Gaussian model. Consequently, the comparison between both models is implicit since we only need to investigate the curves when m equals 1.

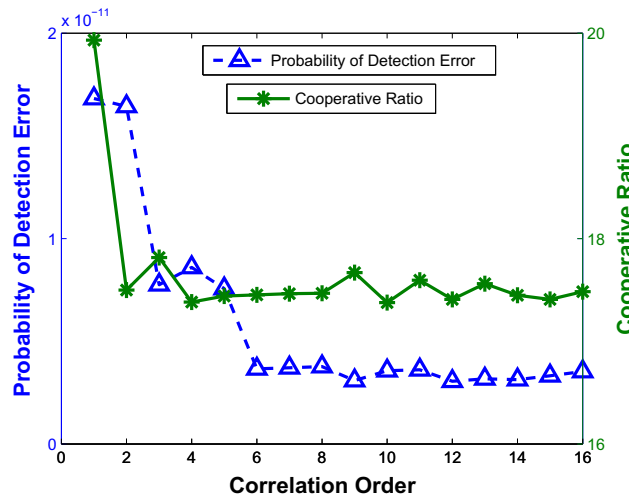
Fig. 8.a plots the average number of hops and the energy consumption as function of m . We can see that the average length of a fusion path decreases as m increases from $n = 38$ when $m = 1$ and drops to 33.5 for $m \geq 2$. The rationale behind this can be explained as follows. Reducing m reduces the amount of information that each node receives from its predecessors. To compensate such drop in the gathered information, additional nodes have to participate in the detection process, which results in an increase of the fusion route length. From an energy consumption point of view, raising m reduces the average length of fusion routes which minimizes the total energy consumption. Note that the energy



(a) Average Number of Hops vs. Energy Consumption.



(b) Chernoff Information vs. Chernoff Efficiency.



(c) Prob. of Detection Error vs. Cooperative Ratio.

Fig. 8. Evaluation of the correlation order impact.

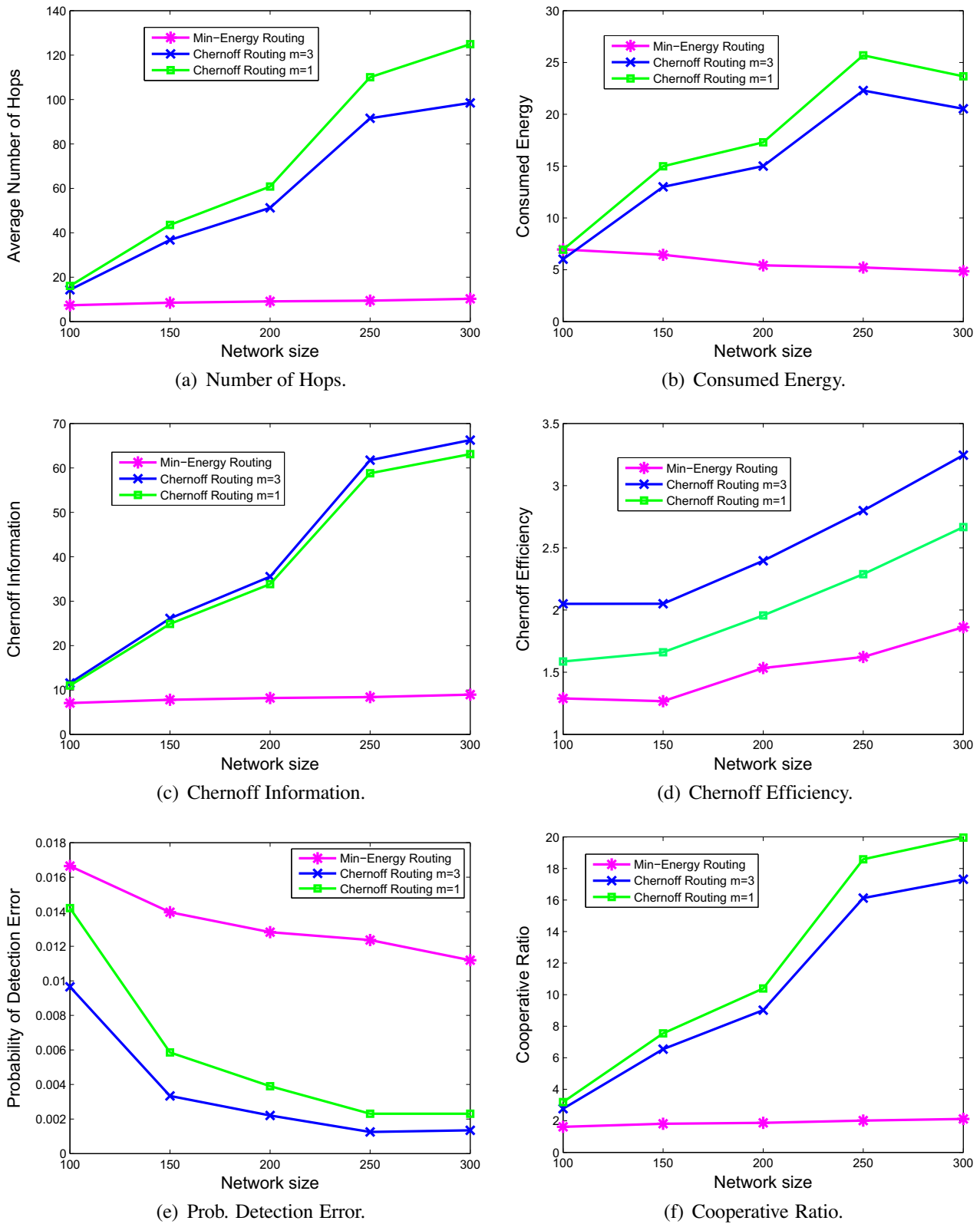


Fig. 9. Evaluation of the network size impact.

consumption decreases by 15% between $m = 1$ and $m = 16$. Indeed, when $m = 1$, the energy consumption equals 4.8 J and drops to 4.2 J when $m \geq 2$.

Fig. 8b shows that the cumulated Chernoff information as well as the Chernoff efficiency increases with m . Increasing m increases

indeed the amount of useful information received at the sink node since each node forwards more information to its successor through the fusion route. Consequently, the probability of detection error will decrease as depicted in Fig. 8c. Note that a 82% decrease in the probability of detection error is achieved between

$m = 1$ and $m = 16$. Moreover, according to Figs. 8a and b, increasing m reduces the total energy consumption and enhances the Chernoff information which justifies the growth in the Chernoff efficiency. The maximum Chernoff efficiency equals 6 when $m = 16$.

Fig. 8c shows the relative improvement in terms of energy-efficiency of our cooperative routing scheme compared to the non-cooperative one, which decreases with m . Recall that decreasing the fusion route length decreases the relative improvement. This explains the decrease of the relative improvement with m since the average fusion route length decreases with m as shown in Fig. 8a.

We would like to emphasize that, according to our study (see Fig. 8), $m = 1$ is the worst case scenario when dealing with our cooperative routing. In fact, we point out that the energy consumption as well as the probability of detection error decrease when m increases. Moreover, the Chernoff information and the Chernoff efficiency increase with m .

Finally, we focus on the comparison between our cooperative routing scheme and the Minimum-Energy scheme. To do so, we consider the worst case scenario ($m = 1$) when dealing with our cooperative routing. Table 2 shows that our proposal provides a Chernoff efficiency improvement by a factor of more than three compared to the Minimum-Energy routing. Moreover, Table 2 shows that our cooperative routing reduces significantly the detection error probability.

7.2.3. Impact of the network size N

We now study the impact of the network size variation on the performance of our cooperative routing scheme considering the cases where $m = 3$ and $m = 3$ while $\omega = 0.8$. Note that, for each network size, the results are averaged over 100 arbitrary generated topologies. Accordingly the following main observations can be made:

- First of all, it is worth noting that Fig. 9 provides a new comparison between the one-dimension Gauss-Markov model ($m = 1$) and our multi-dimension Gaussian Autoregressive model ($m = 3$) under different network size. We would like to emphasize that, Fig. 9 confirms the correlation order study (see Fig. 8). In fact, we point out that, even under various network size, a 3-order Gaussian autoregressive correlation model achieves higher Chernoff efficiency and less detection error probability compared to the one-dimension Gauss-Markov model. **The Chernoff efficiency of our 3-order correlation model is almost 33% greater than the efficiency of the one-order correlation model.** In the following, we focus on the comparison between our cooperative routing scheme ($m = 3$) and the Minimum-Energy scheme.
- Fig. 9.a shows that increasing N increases the average length of a fusion route when our cooperative routing is used. Increasing N enables indeed our cooperative routing to find better routes in terms of detection reliability involving obviously much more nodes.
- The improvement in the detection reliability is depicted in Fig. 9.c where the Chernoff information improves with N , which results in a reduction of detection error probability as shown in Fig. 9.e. Using our cooperative routing scheme ($m = 3$) allows a significant decrease in the probability of detection error. For example, an almost 80% decrease is achieved with our cooperative routing scheme when $N = 200$.
- The above increase in network detection reliability is achieved again at the cost of additional energy consumption as shown in Fig. 9b, where the energy consumption increases with N in the cooperative routing case. **The energy consumption varies between 6 and 22 J.**

- In contrast, the energy consumption decreases with N considering the Minimum-Energy routing case. This is because the cumulative distance of the hops on a fusion route decreases with N and thus the energy consumption decreases. **The energy consumption varies between 7 and 5 J.**
- Fig. 9d shows that our proposal provides always better Chernoff efficiency than Minimum-Energy routing. This indicates that the relative increase of the energy consumption with our scheme is reasonable since it improves significantly the network detection reliability. Recall that, the Chernoff efficiency measures the amount of useful information by one unit of consumed energy ($\text{Chernoff Efficiency} = \frac{\text{Chernoff Information}}{\text{Energy}}$). Fig. 9d shows that The Chernoff efficiency of our cooperative routing is almost 70% greater than the efficiency of the minimum-Energy routing. In other words, for the same amount of consumed energy, we get more useful information with the Chernoff routing protocol. Putting it differently, for the same level of detection reliability, Chernoff routing achieves better energy conservation compared to Minimum-Energy routing.
- Finally, Fig. 9f shows that the relative improvement in terms of energy-efficiency of our cooperative routing scheme compared to the noncooperative one increases with N . This is again due to the increase of the average length of fusion routes with N . **Note that, the energy consumption of the noncooperative routing scheme is almost 18 times the energy consumption of the cooperative routing scheme ($m = 3$) when N is set equal to 300.**

8. Conclusion

In this paper, we studied the use of a detection reliability-aware link metric for routing in wireless sensor networks. Using a generic and realistic multi-dimensional Gaussian autoregressive model to describe the correlation within the supervised field, we derived the expression of a link metric that quantifies the participation of each link on a path in reducing the probability of error when making final decision at the fusion center. Moreover, we used fast filtering to aggregate data information at intermediate nodes along the path to the fusion center. We demonstrated that our cooperative routing scheme enables significant energy conservation compared to conventional Minimum-Energy routing and noncooperative routing schemes for a given detection reliability level. Moreover, we showed that our cooperative routing outperforms the one-dimension Gauss-Markov model in terms of energy-efficiency and the detection reliability. By including a weighted value of the energy consumption in the link cost, we also showed how our cooperative routing can achieve a balance between the detection reliability and energy consumption.

Acknowledgments

This work was supported in part by the Natural Science and Engineering Council of Canada (NSERC) under its Discovery Program and by the World Class University (WCU) Program under the Korea Science and Engineering Foundation funded by the Ministry of Education, Science and Technology (Project No. R31-2008-000-10100-0).

References

- [1] K. Kredon II, P. Mohapatra, Medium access control in wireless sensor networks, *Computer Networks* 51 (4 961–99) (2007).
- [2] J. Deng, Y. Han, W. Heinzelman, P. Varshney, Balanced-energy sleep scheduling in high density cluster-based sensor networks, *Elsevier's Computer Communications Journal* 28 (2005) 1631–1642.

- [3] M. Ali, U. Saif, A. Dunkels, T. Voigt, K. Römer, K. Langendoen, J. Polastre, Z.A. Uzmi, Medium access control issues in sensor networks, *ACM Computer Communication Review (CCR)* 36 (2) (2006) 33–36.
- [4] R.C. Shah, H.M. Rabaey, Energy aware routing for low energy ad hoc sensor networks, *IEEE WCNC*, Orlando, FL, USA, 2002.
- [5] J. Chang, L. Tassiulas, Maximum lifetime routing in wireless sensor networks, *IEEE/ACM Transactions on Networking* 12 (4) (2004) 609–619.
- [6] S. Olariu, I. Stojmenovic, Design guidelines for maximizing lifetime and avoiding energy holes in sensor networks with uniform distribution and uniform reporting, *IEEE INFOCOM*, Barcelona, Spain, April 24–25, 2006.
- [7] F. Bouabdallah, N. Bouabdallah, R. Boutaba, On balancing energy consumption in wireless sensor networks, *IEEE Transactions on Vehicular Technology* 58 (6) (2009) 2909–2924.
- [8] F. Bouabdallah, N. Bouabdallah, R. Boutaba, Towards reliable and efficient reporting in wireless sensor networks, *IEEE Transactions on Mobile Computing* 7 (8) (2008) 978–994.
- [9] M.C. Vuran, I.F. Akyildiz, Spatial correlation-based collaborative medium access control in wireless sensor networks, *IEEE/ACM Transactions on Networking* 14 (2) (2006) 316–329.
- [10] C. Intanagonwiwat, R. Govindan, D. Estrin, Directed diffusion: a scalable and robust communication paradigm for sensor networks, *ACM MOBICOM*, Boston, MA, USA, 2000.
- [11] Y. Sung, S. Misra, L. Tong, A. Ephremides, Cooperative routing for distributed detection in large sensor networks, *IEEE Journal on Selected Areas in Communications* 25 (2) (2007).
- [12] A. Anandkumar, J.E. Yukish, L. Tong, A. Swami, Energy scaling laws for distributed inference in random fusion networks, *IEEE Journal on Selected Areas in Communications* 27 (7) (2009).
- [13] A.S. Ibrahim, Z. Han, K.J.R. Liu, Distributed energy-efficient cooperative routing in wireless networks, *IEEE Transactions Wireless Communications* 7 (10) (2008) 3930–3941.
- [14] J. Zhang, Q. Zhang, Cooperative routing in multi-source multidestination multi-hop wireless networks, in: *Proceedings of IEEE INFOCOM' 2008*, Phoenix, AZ, 2008, pp. 2369–2377.
- [15] Y. Ma, A. Jamalipour, A cooperative cache-based content delivery framework for intermittently connected mobile ad-hoc networks, *IEEE Transactions On Wireless Communications* 9 (1) (2010).
- [16] R. Diversi, R. Guidorzi, Fast filtering of noisy autoregressive signals, *Signal Processing* 87 (2007) 2843–2849.
- [17] S. Appadwedula, V.V. Veeravalli, D.L. Jones, Energy-efficient detection in sensor networks, *IEEE Journal on Selected Areas in Communications* 23 (4) (2005) 693–702.
- [18] T.Q.S. Quek, D. Dardari, M.Z. Win, Energy efficiency of dense wireless sensor networks: to cooperate or not to cooperate, *IEEE Journal on Selected Areas in Communications* 25 (2) (2007) 459–470.
- [19] Y. Yang, R.S. Blum, B.M. Sadler, Energy-efficient routing for signal detection in wireless sensor networks, *IEEE Transactions on Signal Processing* 57 (6) (2009).
- [20] Y. Yang, R.S. Blum, Energy-efficient routing for signal detection under the Neyman-Pearson criterion in wireless sensor networks, *ACM IPSN'07*, Cambridge, Massachusetts, USA, 2007.
- [21] H.V. Poor, *An Introduction to Signal Detection and Estimation*, Springer-Verlag, New York, 1994.
- [22] A. Dembo, O. Zeitouni, *Large Deviations Techniques and Applications*, Springer, 1998.
- [23] P.K. Varshney, C.S. Burrus, *Distributed Detection and Data Fusion*, Springer, 1997.
- [24] B.D.O. Anderson, J.B. Moore, *Optimal Filtering*, Prentice Hall, Englewood Cliffs, NJ, 1979.
- [25] Y. Remion, Décomposition $LDL^T = U^T D U$ incrémentale d'une matrice symétrique, LERL, IUT Léonard de Vinci de Reims.
- [26] F.C. Schwegpe, Evaluation of likelihood functions for Gaussian signals, *IEEE Transactions on Information Theory* 11 (1) (1965) 61–70.